RESEARCH ARTICLE

Clinical and Dopamine Transporter Imaging Trajectories in a Cohort of Parkinson's Disease Patients with GBA Mutations

Silvia Paola Caminiti, PhD,[1,2,3†*] Giulia Carli, MSc,[1,2†] Micol Avenali, MD,[4,5] Fabio Blandini, MD,[4,5] and Daniela Perani, MD[1,2,3]

[1]*School of Psychology, Vita-Salute San Raffaele University, Milan, Italy*
[2]*In Vivo Human Molecular and Structural Neuroimaging Unit, Division of Neuroscience, IRCCS San Raffaele Scientific Institute, Milan, Italy*
[3]*Nuclear Medicine Unit, San Raffaele Hospital, Milan, Italy*
[4]*IRCCS Mondino Foundation, Pavia, Italy*
[5]*Department of Brain and Behavioural Sciences, University of Pavia, Pavia, Italy*

ABSTRACT: Background: Glucosylceramidase (*GBA*) mutations are considered the most common genetic risk factors for developing Parkinson's disease (PD).
Objectives: We aimed to assess, at different time points, the integrity of brain striatal and extra-striatal dopamine pathways and clinical phenotype of a group of PD subjects bearing heterozygous GBA mutations (GBA-PD), compared with a group of idiopathic PD patients (iPD) stratified by age at disease onset. A longitudinal approach was adopted to evaluate the progression over time for clinical and ^{123}I-FP-CIT SPECT imaging features.
Methods: We considered 46 GBA-PD patients and 339 iPD patients, subdivided into two groups according to age at PD onset ($n = 58 < 50$ years and $n = 281 > 50$ years). We measured differences in the occurrence/severity/progression of motor and non-motor features, ^{123}I-FP-CIT standard uptake value ratios (SUVr) in striatal and extra-striatal regions, and global cognitive deterioration over time in a subset of 168 cases with available follow-up.
Results: At baseline, the GBA-PD cohort showed more severe motor and cognitive deficits than the early-iPD cohort. The ^{123}I-FP-CIT SUVr reduction in the striatal and the extra-striatal regions was more marked in the GBA-PD than the early- and late-iPD cohorts. Both GBA-PD and late-iPD patients had a significant annual deterioration in their global cognitive performance, while the early-iPD group showed global cognitive stability over time. At follow-up, the iPD cohorts became similar to the GBA-PD group in ^{123}I-FP-CIT SUVr reduction.
Conclusion: These new findings support the hypothesis of a biological role of GBA mutations in accelerating the early neurodegenerative processes in PD, leading to the malignant clinical phenotype. © 2021 International Parkinson and Movement Disorder Society

Key Words: glucosylceramidase; movement disorder; DAT; cognitive decline; malignant phenotype

Heterozygous mutations in the *GBA* gene, encoding for the lysosomal enzyme glucocerebrosidase (GCase), are considered the most common genetic risk factor for the development of α-synucleinopathies, such as Parkinson's disease (PD) and dementia with Lewy bodies (DLB).[1]

Although the clinical manifestations of GBA-associated PD (GBA-PD) are generally indistinguishable from idiopathic PD (iPD) forms, GBA-PD patients have an earlier disease onset, exhibit faster cognitive deterioration, and lesser benefit from traditional drug interventions than PD patients without GBA mutations.[2-4]

***Correspondence to:** Dr. Silvia Paola Caminiti, Via Olgettina 60, 20132 Milan, Italy; E-mail: caminiti.silviapaola@hsr.it

[†]Authors equally contributing to the manuscript.

Members of the Parkinson's Progression Markers Initiative Investigation are listed in the Appendix.

Funding Agencies: The Parkinson's Progression Markers Initiative—a public–private partnership—is funded by The Michael J. Fox Foundation for Parkinson's Research and funding partners, including AbbVie, Allergan, Avid Radiopharmaceuticals, Biogen, BioLegend, Bristol-Myers Squibb, Celgene, Denali, GE Healthcare, Genentech, GlaxoSmithKline, Lilly, Lundbeck, Merck, Meso Scale Discovery, Pfizer, Piramal, Prevail Therapeutics, Roche, Sanofi Genzyme, Servier, Takeda, Teva, UCB, Verily, Voyager Therapeutics, and Golub Capital, Edmond J. Safra, Handl Therapeutics, Janssen Neuroscience, Neurocrine, Asap.

Received: 20 May 2021; **Revised:** 8 September 2021; **Accepted:** 14 September 2021

Published online 1 October 2021 in Wiley Online Library (wileyonlinelibrary.com). DOI: 10.1002/mds.28818

Age has a central role in the progressive decline of dopaminergic function and the development of PD.[5] Late-onset iPD is associated with greater impairment of dopaminergic function and more rapid disease progression,[6] accompanied by a severe motor and non-motor phenotype and a significant reduction of α-synuclein and total-tau cerebrospinal fluid levels.[7] Conversely, early-onset iPD patients generally have a slower disease progression and more preserved cognitive function.[8] The clinical features found in GBA-PD patients are similar to the "diffuse malignant PD subtype"[9] but with an earlier mean age of onset.

The pathogenetic mechanisms linking GBA mutations to PD are still unknown. It has been proposed that GCase deficiency leads to the accumulation of pathological α-synuclein, which, in turn, inhibits GCase function, thus creating a vicious circle.[10,11]

According to previous studies performed on GBA-PD, the early phase of the disease is phenotypically indistinguishable from the iPD; GBA-PD, however, is characterized by a worse clinical prognosis than iPD.[12-14]

Here, in a large PD cohort (www.ppmi-info.org/database), we considered PD subjects with and without GBA mutations to assess their clinical features at baseline and over time; Moreover, we aimed to evaluate the role of progressive striatal and extra-striatal pathways dysfunction in accelerating phenotypic progression. We compared the GBA-PD cohort with early- and late-onset iPD patients, thus considering the age at disease onset as a variable of interest. We hypothesized that the more malignant clinical progression, characterizing PD-GBA, would be associated with early and severe striatal and extra-striatal pathways dysfunction.

Methods

Participants

Data used in this study were obtained from the Parkinson's Progression Markers Initiative (PPMI) database (www.ppmi-info.org/data), an international, multiple-site, prospective, longitudinal cohort study. The aims and methodology of PPMI have been published elsewhere.[15,16] Study protocols and manuals are available online at www.ppmi-info.org/study-design. The institutional review board approved the study at each site, and the participants provided written informed consent.

We considered the PPMI participants for whom whole exome or genome sequencing was available. The exons 1–11 within the *GBA* gene were Sanger-sequenced and screened for variants. Dual mutation carriers (LRRK2 and GBA) were excluded from this study. GBA variants were also classified according to the mutation's severity[4]: "mild" (N370S [mGBA]), "severe" (L444P, R463C, IVS2 + 1G >A [sGBA]), "risk" (E326K, T369M [rGBA]), and "unknown" (A456P, K(−27)R, R39C, R44C, I489L [uGBA]).

We included 46 PD patients with GBA mutations (GBA-PD) who were drug-naïve and underwent iodine 123 radiolabeled 2β-carbomethoxy-3β-(4-iodophenyl)-N-(3-fluoropropyl) nortropane single-photon emission computed tomography (^{123}I-FP-CIT SPECT) and structural magnetic resonance imaging (MRI) acquisitions at baseline. Drug-naïve iPD patients (N = 339) of the PPMI database with available ^{123}I-FP-CIT SPECT and structural MRI acquisitions at baseline were considered for comparisons of imaging and clinico-demographic characteristics. Specifically, the iPD patients were divided into (i) early-onset iPD, <50 years (n = 58) and (ii) late-onset iPD, >50 years (n = 281).[17-19]

We evaluated the clinical and ^{123}I-FP-CIT standard uptake value ratios (SUVr) rate of change over time in a subset of 168 PD cases with clinical and imaging data available at two follow-up points (GBA-PD = 22, early-iPD = 19 and late-iPD = 127).

We also included 59 healthy controls (HC) (aged 59.19 [10.75] years; 23 females and 36 males), with available MRI and ^{123}I-FP-CIT SPECT acquisitions at baseline for imaging analysis. HC subjects were characterized by normal cognition and motor functionality (Montreal Cognitive Assessment [MoCA] score >26 and Hoehn & Yahr stage = 0). In all HC, ^{123}I-FP-CIT SPECT was rated as negative according to a predefined ranking scale.[20]

Clinical Evaluation

All subjects completed the PPMI standard test battery for motor and non-motor features assessment as described previously.[21,22] See Supplementary Materials S1 for details.

The clinical progression was evaluated by using two different follow-up points. We assessed rates of change by comparing the baseline and the two time points at which all patients received L-dopa treatments, thus controlling for dopaminergic medications. As the first follow-up, we selected a visit at about 2 years, defined as "≈2-years", and a second follow-up as the latest available clinical visit at about 6 years, defined as "≈6-years". Clinical data were acquired in OFF-medications. We investigated the rate of change for clinical markers, calculating the number of points lost per year ([score at follow-up–score at baseline]/years of follow-up).[23]

^{123}I-FP-CIT SPECT Imaging Analysis

Pre-Processing and Analysis of ^{123}I-FP-CIT SPECT Images

The ^{123}I-FP-CIT SPECT and MRI imaging data were retrieved from the PPMI database. See Supplementary Material S2 for a description of pre-processing procedures.

^{123}I-FP-CIT SUVr (the parameter of interest) was calculated as [(target region/reference region)−1] for each subject-specific region of interest (ROI) (Supplementary Materials S3). The lateral superior occipital cortex uptake was used as the background reference region.

We extracted mean SUVr values from left and right putamen to identify the predominant side of dopamine transporter (DAT) SUVr defect in each PD patient, then, we computed a DAT SUVr asymmetry index (AI).[24] According to the AI,[24] the SUVr values for all selected ROIs were flipped ROI-by-ROI, setting the hemisphere with the lower SUVr on the left side. These ipsilateral (left) and contralateral (right) uptake values were employed for the statistical analyses (Fig. 1).

We evaluated the rates of change for regional SUVr values across the groups, from baseline to "≈2-years" visit; we selected the "≈2-years" visit to include the largest number of subjects with ^{123}I-FP-CIT SPECT available (GBA-PD = 16, early-iPD = 17, and late-iPD = 74). Rates of change for imaging data were obtained as described for clinical data.[23] Imaging data were acquired in OFF-medications.

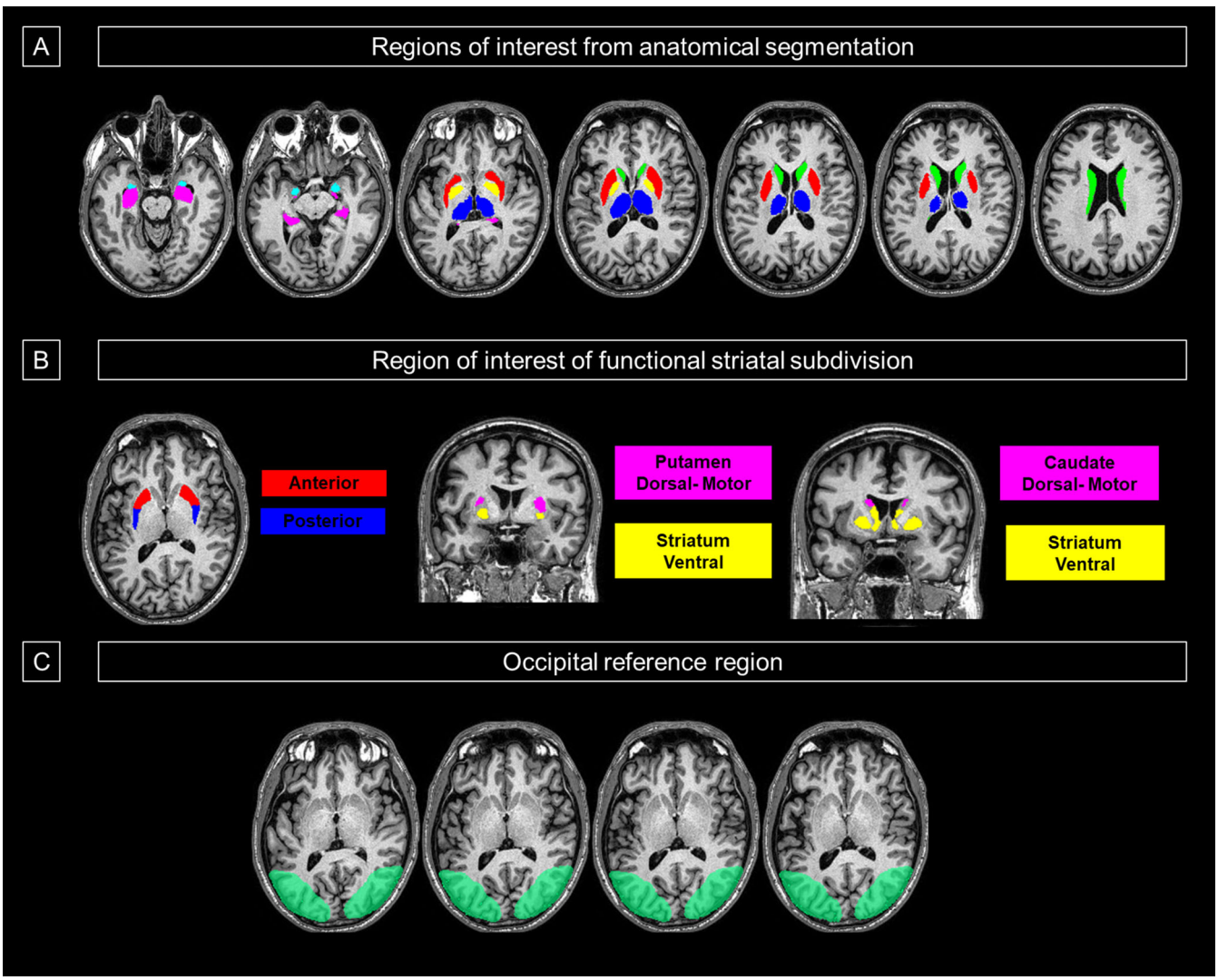

FIG. 1. Subject-specific regions of interest (ROIs). Example of anatomical subject-specific ROIs superimposed on the relative magnetic resonance imaging (MRI)-T1 image in the native space of a glucosylceramidase-associated Parkinson's disease (GBA-PD) patient. (**A**) ROIs obtained by the automatic anatomical segmentation of MRI scan, performed using volbrain. Twelve bilateral ROIs were defined in each subject: whole caudate nucleus (green), whole putamen (red), globus pallidus (dark yellow), thalamus (blue), hippocampus (pink), and amygdala (light blue). (**B**) The functional striatal subdivision following literature guidelines. The right panel shows the anterior (red) and posterior (blue) subdivisions of the whole putamen. The boundary between the anterior and posterior putamen was taken to be the posterior aspect of the fornix. The left panel shows a functional subdivision of the striatum based on a multimodal imaging study.[25] The functional subdivision of the striatum includes dorsal-motor (pink) and ventral (yellow) divisions. (**C**) This panel displays the lateral superior occipital cortex ROI used as the background reference region to calculate standard uptake value ratio (SUVr) values. [Color figure can be viewed at wileyonlinelibrary.com]

Statistical Analyses

MANCOVA and ANOVA with Bonferroni correction for normally distributed variables and Kruskal–Wallis with Bonferroni correction for non-parametric variables were used to compare demographics, clinical, and imaging data. We considered the following confounding variables for clinical measures comparisons among PD groups: (i) gender and disease duration for baseline evaluation comparisons and (ii) gender, disease duration, and levodopa equivalent daily dose (LEDD) for follow-up comparisons. Statistical analysis comparing the brain structural volumes among the different groups were adjusted for gender, Unified Parkinson's Disease Rating Scale-Part III (UPDRS-III) and disease duration. Gender, disease duration, ROIs structural volumes, and UPDRS-III were used as nuisance variables for all the ^{123}I-FP-CIT imaging comparisons. In both individual and the whole clinical groups (i.e., GBA-PD and early-/late-iPD groups pooled together), we assessed the prediction of ^{123}I-FP-CIT SUVr at baseline for all the considered ROIs

TABLE 1 *Clinical and demographic features at baseline*

Feature	GBA-PD (N = 46) Mean (SD)	Early-iPD (N = 58) Mean (SD)	Late-iPD (N = 281) Mean (SD)	F-statistic[a]	T-statistic[a] GBA-PD vs. early-iPD	GBA-PD vs. late-iPD	Early-iPD vs. late-iPD
Gender (M/F)	26/20	33/25	193/88	$P = 0.091$	–		
Age at onset (years)	57.4 (10)	44.5 (5.5)	63.6 (7.0)	$P = \mathbf{0.000}$	$P = \mathbf{0.000}$	$P = \mathbf{0.001}$	$P = \mathbf{0.000}$
Age at baseline (years)	58.9 (9.6)	47 (4.8)	64.8 (7.1)	$P = \mathbf{0.000}$	$P = \mathbf{0.001}$	$P = \mathbf{0.000}$	$P = \mathbf{0.000}$
Age (years; min–max)	29–81	33–54	51–84	–	–	–	–
Education (years)	15.9 (2.9)	15.7 (2.8)	15.4 (3.1)	$P = 0.333$	–	–	–
Disease duration (years)	1.5 (1.4)	2.5 (3.2)	1.3 (1.6)	$P = \mathbf{0.003}$	$P = 0.441$	$P = 0.693$	$P = \mathbf{0.003}$
Hoehn & Yahr scale[b]	1.9 (0.3)	1.6 (0.5)	1.8 (0.6)	$P = \mathbf{0.001}$	$P = \mathbf{0.002}$	$P = 0.673$	$P = \mathbf{0.003}$
UPDRS Part III[b]	28.9 (10.2)	21.7 (10.8)	26.7 (12.2)	$P = \mathbf{0.002}$	$P = \mathbf{0.003}$	$P = 0.654$	$P = \mathbf{0.006}$
UPDRS total score[b]	41.5 (12.6)	33.7 (16)	38.0 (15.6)	$P = \mathbf{0.012}$	$P = \mathbf{0.013}$	$P = 0.516$	$P = 0.057$
MoCA total score[b]	26.9 (2.5)	28.1 (2.3)	27.0 (2.3)	$P = \mathbf{0.003}$	$P = \mathbf{0.016}$	$P = 1.000$	$P = \mathbf{0.004}$
SCOPA-AUT total score[b]	15.7 (12.4)	11.4 (7.8)	14.1 (9.4)	$P = \mathbf{0.004}$	$P = \mathbf{0.017}$	$P = 1.000$	$P = \mathbf{0.006}$
RBDSQ score[b]	4.4 (3.0)	3 (2.3)	3.1 (2.6)	$P = \mathbf{0.004}$	$P = \mathbf{0.027}$	$P = \mathbf{0.003}$	$P = 1.000$
UPSIT score[b]	21.9 (8.2)	25.1 (7.7)	21.6 (8.2)	$P = 0.082$	$P = 0.206$	$P = 1.000$	$P = 0.098$

Abbreviations: GBA, glucosylceramidase beta; PD, Parkinson's disease; i, idiopathic; SD, standard deviation; M, male; F, female; UPDRS, Unified Parkinson's Disease Rating Scale; MoCA, Montreal Cognitive Assessment; RBDSQ, Rapid Eye Movement Sleep Behavior Disorder Screening Questionnaire; SCOPA-AUT, Scales for Outcomes in Parkinson's Disease—Autonomic dysfunction; UPSIT, University of Pennsylvania Smell Identification Test. Bold letters indicate P value < 0.05.

[a]Corrected for Bonferroni.

[b]Controlled for disease duration and gender.

on the degree of clinical deterioration (i.e., rate of change of all clinical variables from "≈2-years" to "≈6-years" follow-up) through linear regression analyses. In the same groups, we also calculated the correlation among these clinical and imaging measures. We considered ROIs structural volumes, disease duration, LEDD, and gender as nuisance variables. SPSS 26.0 software was used for statistical analysis.

Results

Baseline and follow-up demographic, clinical, and ^{123}I-FP-CIT imaging features are reported in Table 1 and Tables S2–S5.

In the GBA-PD group, 63% (29/46) of patients carried rGBA, 9% (4/46) sGBA, 15% (7/46) mGBA, and 13% uGBA (6/46) variants.

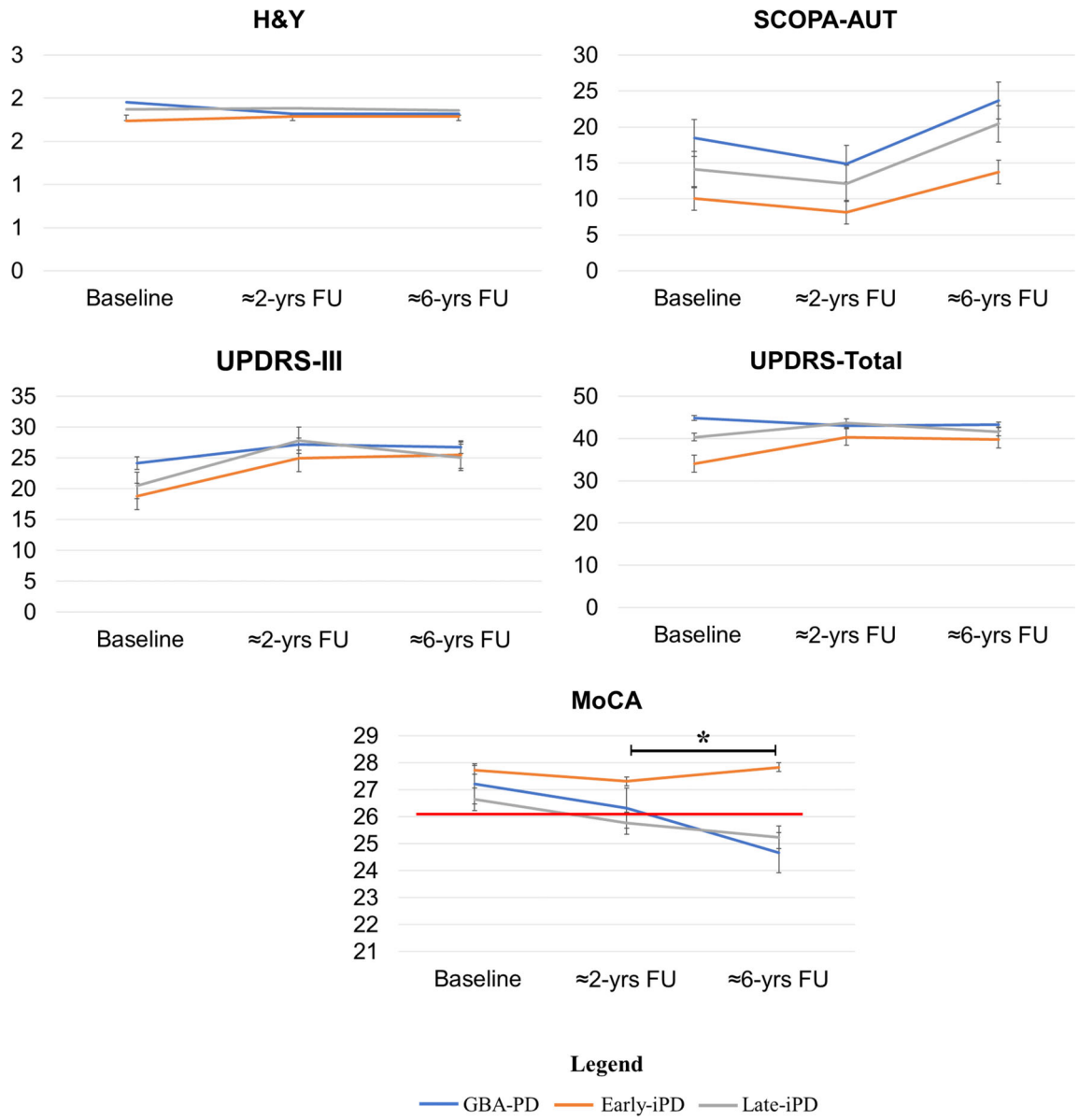

FIG. 2. Clinical and global cognitive progression of glucosylceramidase-associated Parkinson's disease (GBA-PD) and idiopathic PD (iPD) subgroups at three time points. Longitudinal changes in outcomes of interest in different PD groups (GBA-PD = 22; early-iPD = 19, and late-iPD = 127), (GBA-PD in blue, early-iPD in orange, and late-iPD in grey) with longitudinal data at three time points. Mean follow-up duration in the entire population at early follow-up = 1.74 years and last available follow-up = 6.40 years. The red line in the MoCA panel represents the clinical cut-off. *Significant statistical differences in clinical progression. The dark line represents the longitudinal time frame from 2 to 6 years follow-up. GBA-PD showed a significantly faster global cognitive deterioration than the early-iPD group from "≈2-years" to "≈6-years" visits (P = 0.043). H&Y, Hoehn & Yahr; SCOPA-AUT, Scales for Outcomes in Parkinson's disease – Autonomic dysfunction; FU, follow-up; Yrs, years; UPDRS-III, Unified Parkinson's Disease Rating Scale-Part III; MoCA, Montreal Cognitive Assessment. [Color figure can be viewed at wileyonlinelibrary.com]

Cross-Sectional Study

Clinical and Global Cognitive Features

Baseline - The GBA-PD group showed significantly higher Hoehn & Yahr, UPDRS-III, UPDRS total, and SCOPA-AUT scores than early-iPD, but these were not different from late-iPD. The GBA-PD group also had higher Rapid Eye Movement Sleep Behavior Disorder Screening Questionnaire (RBDSQ) scores than both the early-iPD and late-iPD groups. MoCA scores were lower than the early-iPD but comparable to the late-iPD (Table 1).

"2-years" follow-up - The GBA-PD and late-iPD groups showed significantly higher SCOPA-AUT scores than early-iPD (Table S2).

"6-years" follow-up - The GBA-PD group presented significantly more severe UPDRS-III and MoCA scores than early-iPD (Table S3).

Imaging Features

The analysis of brain structural volumes revealed statistically significant differences among groups. Compared with the early-iPD group, more prevalent structural volume reductions were observed in the brains of late-iPD and GBA-PD groups than the early-iPD group. In particular, the comparison between early- and late-iPD showed significant differences in 18 of 22 ROIs and between early-iPD and GBA-PD in 12 of 22 ROIs (Table S1).

The PD-GBA, early-iPD, and late-iPD patients shared significantly decreased ^{123}I-FP-CIT SUVr than the HC in all the considered ROIs, except for the ventral striatum, hippocampus, and amygdala, bilaterally. GBA-PD patients showed a significantly lower DAT SUVr in the bilateral ventral striatum than HC and early-iPD and late-iPD. The GBA-PD group showed a significantly lower ^{123}I-FP-CIT SUVr in the whole contralateral putamen, anterior and motor putamen, globus pallidus, hippocampus, and amygdala than the early-iPD group. All the significant differences in ^{123}I-FP-CIT SUVr among clinical groups are shown in Fig. 3 and Table S4.

At the "≈2-years" follow-up visit, no statistically significant differences emerged among groups (Table S5).

Longitudinal Progression Study

Clinical and Global Cognitive Features

The longitudinal progression analysis from "≈2-years" to "≈6-years" visits showed a significantly faster global cognitive deterioration in the GBA-PD group than the early-iPD group ($P = 0.043$). Over this follow-up period, GBA-PD patients lost 0.29 MoCA points per year, and early-iPD patients remained stable

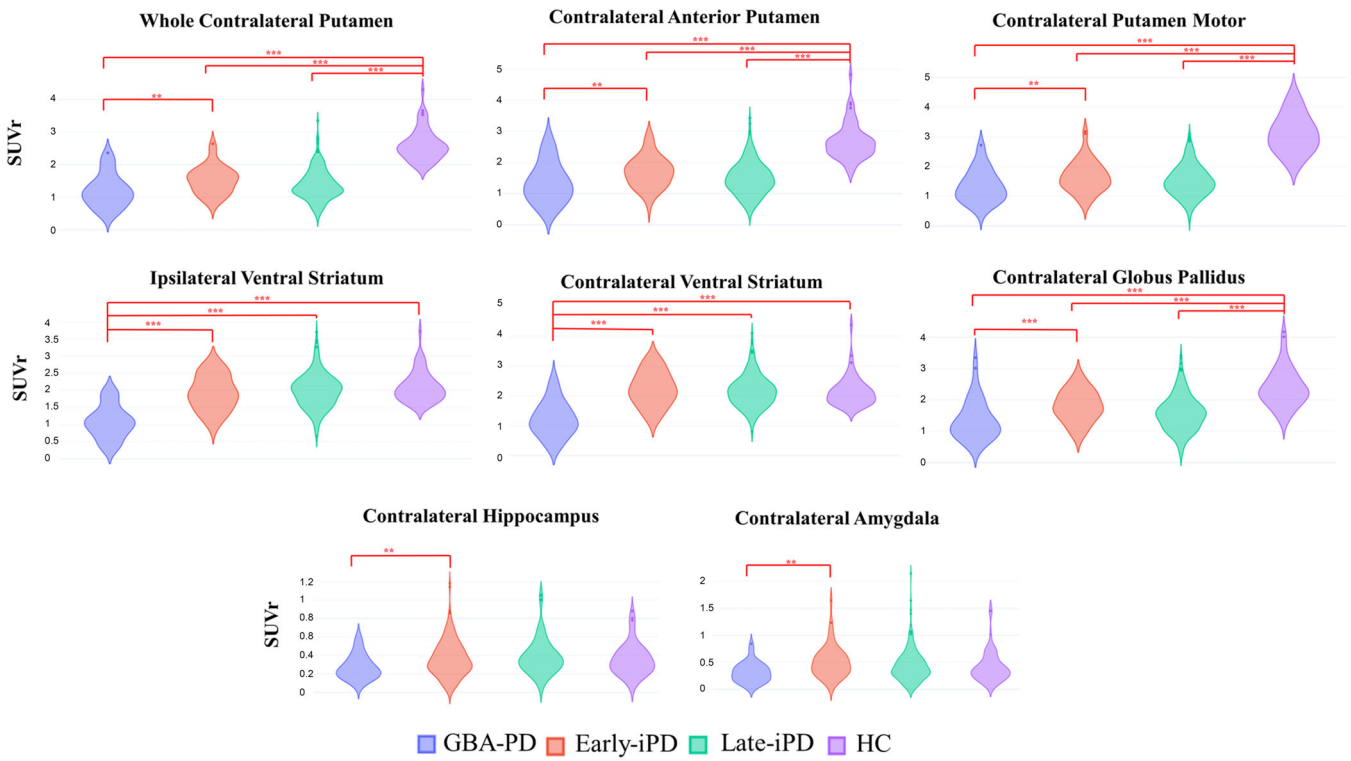

FIG. 3. Differences in ^{123}I-FP-CIT imaging standard uptake value ratio (SUVr) at baseline. Panel with violin plots depicting significant differences in ^{123}I-FP-CIT SUVr data of regions of interest (ROIs) in the four considered clinical groups: glucosylceramidase-associated Parkinson's disease (GBA-PD) (purple), early idiopathic Parkinson's disease (early-iPD) (orange), late-iPD (green), and healthy controls (HC) (violet). ***Statistical difference at $P < 0.000$. **Statistical difference at $P < 0.05$. [Color figure can be viewed at wileyonlinelibrary.com]

(Fig. 2). The late-iPD group lost 0.08 points per year of MoCA from "≈2-years" to "≈6-years" follow-up visits. Of note, at "≈6-years" follow-up, the 10% of GBA-PD and the 17% of late-iPD patients were below the MoCA cut-off score of 26, with 1.63 MoCA points lost per year in GBA-PD and 1.34 points lost per year in late-iPD. The 75% (3/4) of sGBA genotype moved from normal to pathological MoCA values from baseline to "≈6-years" visit. The early-iPD group was instead stable over time (Fig. 2 and Table S6). The three groups had no significant differences in rates of change of the other considered clinical variables.

Imaging Features

From baseline to "≈2-years" follow-up, we found that the GBA-PD showed a global SUVr rate of change (i.e., mean rate of change of all considered ROIs) equal to −0.11, early-iPD equal to −0.09, and late-iPD equal to −0.16 (Fig. 4). The late-iPD group showed the highest global SUVr rate of change. Of note, we found that the early-iPD and late-iPD groups significantly increased their SUVr rate of change, namely significant SUVr reductions over time, in the ventral striatum in comparison with the GBA-PD group at "≈2-years" (early-iPD vs. GBA-PD $P = 0.024$; late-iPD vs. GBA-PD $P < 0.001$).

Relationship between Motor and ^{123}I-FP-CIT SPECT Measures

We found a significant correlation between low SUVr values in the thalamus at baseline and MOCA worsening from "≈2-years" to "≈6-years" follow-up visits in the early-iPD group ($r = 0.996$; $P = 0.034$). The linear regression model revealed that low SUVr values in the caudate nucleus (motor division) at baseline were associated with UPDRS-III motor scores worsening from "≈2-years" to "≈6-years" follow-up visits in the whole PD patients ($B = -6.46$; $P = 0.021$) and in the late-iPD group ($B = -10.26$; $P = 0.009$).

In the whole PD group (385 patients), we found that 254 (66.75%) patients were classified as having motor asymmetry (0.30 < motor asymmetry index < −0.30). The mean (SD, range) side-to-side difference in UPDRS-III was 9.18 points (3.6, 1–20). Similarly, 311 of 385 (80.78%) patients were classified as having dopaminergic asymmetry (0.05 < asymmetry index < −0.05). The mean (SD, range) relative side-to-side difference in putamen SUVr was 37.8% (22.7, 5.4–150.20) in these patients. Finally, 219 patients (56.88%) were classified as having both a motor and dopaminergic asymmetry and, among these, 90% showed consistent clinical and imaging laterality.

Twenty-one of 46 patients (45.65%) showed DAT SUVr asymmetry and motor asymmetry in the GBA-PD group. In the early-iPD group, 43 of 58 patients (74.14%) showed DAT SUVr asymmetry and motor asymmetry. In the late-iPD group, 155 of 218 patients (55.16%) showed DAT SUVr asymmetry and motor asymmetry.

When the three groups were compared for their DAT SUVr and motor asymmetry characteristics, differences emerged ($\chi^2 = 9.747$; $P = 0.008$), where GBA-PD (45.65%) and late-iPD (55.16%) patients showed less DAT SUVr and motor asymmetry than the early-iPD group (74.14%).

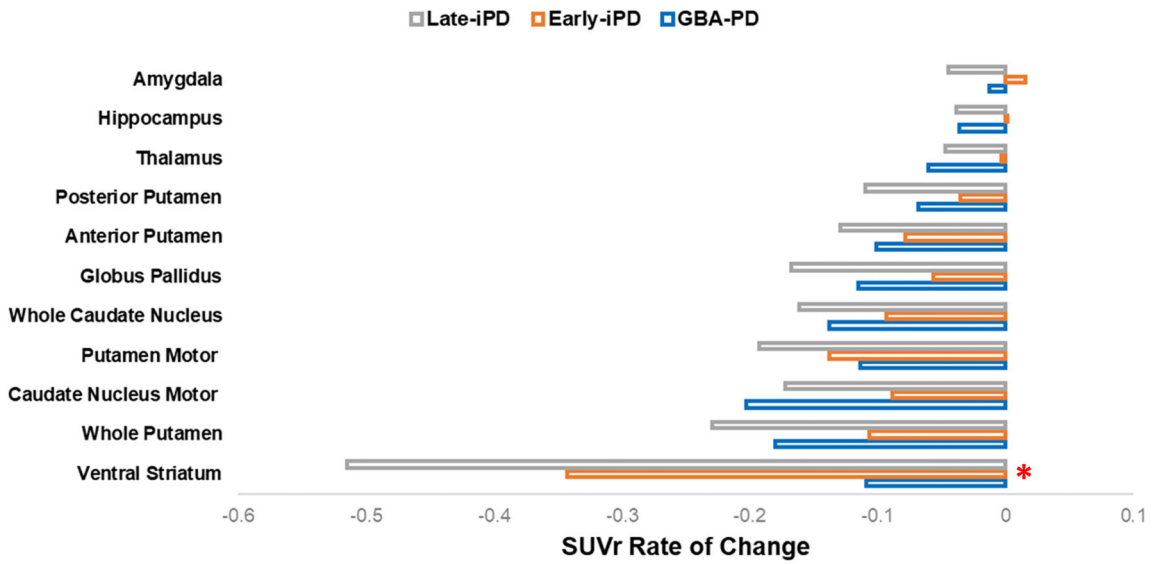

FIG. 4. Rate of changes of ^{123}I-FP-CIT standard uptake value ratio (SUVr). Horizontal bar plot depicting the rate of changes per year of ^{123}I-FP-CIT SUVr data extracted from subject-specific regions of interest in each Parkinson's disease (PD) group (glucosylceramidase-associated Parkinson's disease [GBA-PD] in blue, early idiopathic Parkinson's disease [early-iPD] in orange, and late-iPD in grey). *Late- and early-iPD groups showed a significantly higher rate of change in the ventral striatum than GBA-PD, already severely affected. [Color figure can be viewed at wileyonlinelibrary.com]

Discussion

The current study evaluated clinical features and ^{123}I-FP-CIT imaging in a large population of drug-naïve PD patients with GBA mutations, comparing them for the first time with two cohorts of drug-naïve iPD stratified by their age at symptoms onset, with a combined cross-sectional and longitudinal design.

Limited evidence reports DAT imaging results in GBA-PD carriers, with significant increases[14] or decreases[13] of dopaminergic activity in GBA-PD compared to iPD. Specifically, these studies investigated ^{123}I-FP-CIT imaging in GBA-PD compared to iPD, focusing analyses only on putamen and caudate nucleus without stratifying the cohorts according to age at symptoms onset.[13,14] Our study applied a comprehensive approach comparing GBA-PD and iPD stratified according to the age of onset and evaluating ^{123}I-FP-CIT SUVr in striatal and extra-striatal targets.[25-28] On a methodological note, our findings are based on a subject-specific ROI approach based on the structure segmentation of MRI scans in each participant. The automatic delineation of anatomical structures derived from single-subject structural T1-weighted MRI images and the introduction of MRI-ROI volumetrics as a nuisance variable increases the precision of ^{123}I-FP-CIT SUVr extraction. Furthermore, introducing the MRI-ROI volumetrics as a nuisance variable made the results more solid, as the GBA-PD and late-iPD groups showed significantly lower MRI-ROI volumes than the early-iPD group in the majority of considered ROIs (Table S1). The structural data results highlight degenerative processes and neuronal death in the structures of the dopaminergic pathways since the early phase of PD.

Our results (both cross-sectional and longitudinal ones) suggest that GBA mutations accelerate the neurodegenerative processes, leading to significant dopaminergic damage and a more severe clinical phenotype, already at the beginning of the disease. Specifically, the cross-sectional analysis at baseline, indicating the early involvement of dorsal and ventral striatum in the GBA-PD group, supports the hypothesis of a more extended biological effect of the GBA mutations than the idiopathic forms on the dopaminergic systems (Table S4 and Fig. 3). The longitudinal evaluation demonstrated that after only 2 years, both early- and late-iPD groups reached the same dopaminergic damage severity as GBA-PD patients in the ventral striatum (Fig. 4).

Late-iPD and GBA-PD showed a comparable clinical and cognitive deterioration, compatible with the definition of "diffuse malignant" PD clinical phenotype, contrary to the early-iPD showing a stable global cognitive course (Fig. 2). Our findings support the hypothesis that early-iPD represents a PD clinical condition characterized by a slow disease course and stable cognitive progression.

According to the literature, the PD malignant phenotype is usually characterized by more severe motor and non-motor symptoms, more significant atrophy of the substantia nigra area, and more dopaminergic deficits in SPECT.[29] The key clinical markers of a malignant subtype are RBD, autonomic dysfunctions, and rapid progression to severe cognitive impairment.[9,30] In the present series, the GBA-PD group also showed higher RBDSQ scores than the two iPD groups, suggesting a higher prevalence of sleep disorder in the GBA-PD cohort. RBD in PD subjects is considered a marker of a more malignant phenotype, with a faster motor and non-motor symptoms progression.[29] RBD in PD is also related to the diffusion and severe deposition of synuclein at autopsy.[31]

The malignant PD is characterized by a more rapid decline in global cognition (a progressive worsening of MoCA scores).[29] Accordingly, in our study GBA-PD and the late-iPD patients lost more than 1 MoCA point per year, while the early-iPD cases showed global cognitive stability during the years (Fig. 2 and Table S6). Our report found that after 6 years, the 10% of GBA-PD and the 17% of late-iPD patients were below the MoCA cut-off score of 26, with 1.63 MoCA points lost per year in GBA-PD and 1.34 points lost per year in late-iPD. Conversely the early-iPD group was stable. A large study including 421 individuals with de novo early PD found that the "malignant" phenotype lost 1.8 points in a mean follow-up time of 2.9 years.[29]

Previous studies suggest that GBA mutations have a biological effect on a more aggressive PD phenotype.[13,32] Even if in a limited number of patients, we found that the severe GBA variant showed faster cognitive deterioration, consistent with recent evidence reporting that patients with severe GBA-PD mutations had the highest burden of cognitive impairment.[4] Future studies with large samples of GBA-PD patients with clinical and neuroimaging data available are needed to provide solid evidence for the role of specific GBA variants—especially T369M and variants of unknown significance, in the expression of clinical phenotypes.

The DAT activity comparison with HC revealed a dopaminergic impairment in almost all nigrostriatal structures affecting three PD cohorts—GBA-PD, late-iPD, and early-iPD (Table S1). In the ventral striatum, at baseline, only GBA-PD showed decreased DAT activity. De novo late-iPD and early-iPD patients, instead, showed levels of DAT activity comparable with HC at baseline. After about a 2-year follow-up, early-iPD and late-iPD groups showed a rapid decrease of ^{123}I-FP-CIT SUVr in the ventral striatum (Fig. 4). Notably, the SUVr in the ventral striatum was significantly lower in the GBA-PD group than the idiopathic-PD groups at baseline (Table S1) but

became comparable to the other groups after a 2-year follow-up (Table S3). Our results suggest that GBA mutation is associated with accelerated neurodegenerative processes, leading to a severe ^{123}I-FP-CIT SUVr reduction in the GBA-PD group already at the beginning of the disease. The ventral striatum receives projections from the ventral tegmental area neurons, and it is part of the dopaminergic mesolimbic system.[25] Early PD pathology involves the dorsal-motor striatum and spares the ventral striatum and the ventral tegmental area.[33] However, during the disease course, the mesolimbic system is unequivocally affected by PD pathology.[34] The early involvement of ventral striatum in the GBA-PD group further supports the hypothesis about the role of GBA mutations in causing severe and more extended dopaminergic damage than the idiopathic forms.

The GBA-PD group had significantly reduced ^{123}I-FP-CIT SUVr in the globus pallidus, hippocampus, and amygdala compared with the early-iPD cohort, comparable to the late-iPD (Table S1). Previous reports investigated extra-striatal ^{123}I-FP-CIT SUVr in iPD. Kaasinen et al reported decreased SUVr in the olfactory cortex, thalamus, and anterior cingulate cortex in PD compared to controls.[24] Pilotto et al recently reported a significant SUVr reduction in the thalamus and insula in PD compared to controls.[35] Of note, our study is the first attempt to explore this issue in a group of well-characterized newly diagnosed GBA-PD and compare them with two groups of iPD patients. Alterations of extra-striatal ^{123}I-FP-CIT SUVr are involved in different phenotypes of iPD[36] and are associated with the severity of motor symptoms and decline of cognitive performance.[37,38]

No significant correlation was found between regional ^{123}I-FP-CIT SPECT SUVr values and clinical measures at baseline. Considering that PD's earliest clinical motor manifestations occur at the point of at least a 50% loss of dopaminergic transporter SUVr,[39,40] our results are not surprising. A significant correlation between imaging and clinical variables emerged when we considered the clinical progression at "≈2-years" and "≈6-years" follow-up. Low SUVr values in the motor division of the caudate nucleus at baseline were associated with worsening motor scores from "≈2-years" to "≈6-years" visits in the whole PD group and late-iPD clinical group. Thus, the presynaptic dopamine depletion in the caudate nucleus motor division in the de novo stage predicted the later severity of motor symptoms in the whole PD and late-PD groups using longitudinal data. It should be acknowledged that the UPDRS-III scores characterizing the three cohorts of patients remained almost unchanged over time (Fig. 2). The current evidence may be related to the effects of therapeutic interventions slowing the progression of motor deficits and making the rate of change stable over time.

Unfortunately, in this study the ^{123}I-FP-CIT imaging data at "≈6-years" were not available in a sufficient number of subjects to evaluate pathological trajectories over a longer time frame. Our ^{123}I-FP-CIT imaging finding, comparing baseline with "≈2-years" data, suggests that the dopaminergic damage reached plateau faster in the GBA-PD cohort than in the iPD groups. Moreover, the GBA-PD group showed more widespread dopaminergic damage since the early clinical phases, supported by the lack of dopaminergic asymmetry.

The evidence of lower DAT density in patients with diffuse brain Lewy bodies disease (PDD/DLB) compared to PD patients with mild motor-predominant phenotype[13,41] suggests that within the clinical spectrum of PD, patients with GBA mutations are much closer to the diffuse malignant phenotype (PDD/DLB).

How GBA mutations produce an effect on DA integrity is still unclear. Glycosylceramide—the substrate of GCase—may cause the accumulation of α-synuclein and, conversely, the accumulation of α-synuclein may lead to a decrease in GCase activity.[10] Overexpression of α-synuclein led to reduced GCase levels in brain tissue,[42,43] cerebrospinal fluid,[44] and peripheral blood of PD patients.[45,46] Furthermore, by targeting mitochondria and endoplasmic reticulum functions, GCase defects impact cellular energy production and proteostasis; more importantly, GCase deficiency is associated with remarkable microglia activation, which points to neuroinflammation as another major consequence of GBA mutations.[47] All in all, these studies indicate a malignant neurotoxic cycle that GBA mutations may trigger. The reason for the vulnerability of specific neuron types, however, is still not clarified. One potential mechanism could be the increased levels of α-synuclein in synaptic DA terminals, where the a-synuclein oligomeric forms start the degenerative process.[48] Specific neurons are vulnerable to α-synuclein pathology,[49] and these neurons share morphological traits, namely the presence of long and highly branched axons with a considerable number of transmitter release sites. The neurons with these characteristics are the dopaminergic neurons arising from the substantia nigra and projecting to the striatum.[50] Accordingly, post-mortem evidence demonstrated a widespread deficiency of GCase activity in GBA-PD brains, with the most severe defect located in the substantia nigra (58%) and putamen (48%).[51]

In conclusion, our findings confirm that the GBA mutations contribute to a more severe phenotype in motor staging and global cognitive decline[52,53] with an underlying widespread and severe nigrostriatal, mesolimbic, and extra-striatal SUVr deficiency.

Future studies will be necessary, focusing on factors such as the co-existence of α-synuclein, tau, and amyloid proteinopathies or/and the differential proxies of cognitive and brain reserve together with GBA

mutations in modulating disease progression. Moreover, a large follow-up sample size addressing the clinical effects of GBA variants may reveal their role in determining the malignant phenotype.

Acknowledgments: Data used in the preparation of this article were obtained from the Parkinson's Progression Markers Initiative database (www.ppmi-info.org/data). For up-to-date information on the study, visit www.ppmi-info.org. We thank Cristina Tassorelli, Anna Sofia Resta, and Edoardo De Natale for their valuable support.

Data Availability Statement

Data used in the preparation of this article were obtained from the Parkinson's Progression Markers Initiative database (www.ppmi-info.org/data). For up-to-date information on the study, visit www.ppmi-info.org.

References

1. Neumann J, Bras J, Deas E, et al. Glucocerebrosidase mutations in clinical and pathologically proven Parkinson's disease. Brain 2009; 132:1783–1794.
2. Tayebi N, Walker J, Stubblefield B, et al. Gaucher disease with parkinsonian manifestations: does glucocerebrosidase deficiency contribute to a vulnerability to parkinsonism? Mol Genet Metab 2003; 79:104–109.
3. Ryan E, Seehra G, Sharma P, Sidransky E. GBA1-associated parkinsonism: new insights and therapeutic opportunities. Curr Opin Neurol LWW 2019;32:589–596.
4. Petrucci S, Ginevrino M, Trezzi I, et al. GBA-related Parkinson's disease: dissection of genotype–phenotype correlates in a large Italian cohort. Mov Disord 2020;35:2106–2111.
5. Critchley M. The neurology of old age. Lancet 1931;217: 1119–1127.
6. Van Rooden SM, Heiser WJ, Kok JN, Verbaan D, Van Hilten JJ, Marinus J. The identification of Parkinson's disease subtypes using cluster analysis: a systematic review. Mov Disord 2010;25:969–978.
7. Pagano G, Ferrara N, Brooks DJ, Pavese N. Age at onset and Parkinson disease phenotype. Neurology 2016;86:1400–1407.
8. Schrag A, Schott JM. Epidemiological, clinical, and genetic characteristics of early-onset parkinsonism. Lancet Neurol 2006;5: 355–363.
9. Fereshtehnejad S-M, Romenets SR, Anang JBM, Latreille V, Gagnon J-F, Postuma RB. New clinical subtypes of Parkinson disease and their longitudinal progression: a prospective cohort comparison with other phenotypes. JAMA Neurol 2015;72:863–873.
10. Mazzulli JR, Xu YH, Sun Y, et al. Gaucher disease glucocerebrosidase and α-synuclein form a bidirectional pathogenic loop in synucleinopathies. Cell 2011;146:37–52.
11. Schapira AHV. Glucocerebrosidase and Parkinson disease: recent advances. Mol Cell Neurosci 2015;66:37–42.
12. Adler CH, Beach TG, Shill HA, et al. GBA mutations in Parkinson disease: earlier death but similar neuropathological features. Eur J Neurol 2017;24:1363–1368.
13. Cilia R, Tunesi S, Marotta G, et al. Survival and dementia in GBA-associated Parkinson's disease: the mutation matters. Ann Neurol 2016;80:662–673.
14. Simuni T, Brumm MC, Uribe L, et al. Clinical and dopamine transporter imaging characteristics of leucine rich repeat kinase 2 (LRRK2) and glucosylceramidase beta (GBA) Parkinson's disease participants in the Parkinson's progression markers initiative: a cross-sectional study. Mov Disord 2020;35:833–844.
15. Marek K, Jennings D, Lasch S, et al. The Parkinson Progression Marker Initiative (PPMI). Prog Neurobiol 2011;95:629–635.
16. Marek K, Chowdhury S, Siderowf A, et al. The Parkinson's Progression Markers Initiative (PPMI)–establishing a PD biomarker cohort. Ann Clin Transl Neurol 2018;5:1460–1477.
17. Chen Y, Gu X, Ou R, et al. Evaluating the role of SNCA, LRRK2, and GBA in Chinese patients with early-onset Parkinson's disease. Mov Disord 2020;35:2046–2055.
18. Schirinzi T, Di Lazzaro G, Sancesario GM, et al. Young-onset and late-onset Parkinson's disease exhibit a different profile of fluid biomarkers and clinical features. Neurobiol Aging 2020;90:119–124.
19. Willis AW, Schootman M, Kung N, Racette BA. Epidemiology and neuropsychiatric manifestations of young onset Parkinson's disease in the United States. Parkinsonism Relat Disord 2013;19:202–206.
20. Darcourt J, Booij J, Tatsch K, et al. EANM procedure guidelines for brain neurotransmission SPECT using 123 I-labelled dopamine transporter ligands, version 2. Eur J Nucl Med Mol Imaging 2010; 37:443–450.
21. Malek N, Weil RS, Bresner C, et al. Features of *GBA*-associated Parkinson's disease at presentation in the UK *Tracking Parkinson's* study. J Neurol Neurosurg Psychiatry 2018;89:702–709.
22. Lerche S, Schulte C, Srulijes K, et al. Cognitive impairment in Glucocerebrosidase (GBA)-associated PD: not primarily associated with cerebrospinal fluid Abeta and tau profiles. Mov Disord 2017; 32:1780–1783.
23. Caroli A, Prestia A, Galluzzi S, et al. Mild cognitive impairment with suspected nonamyloid pathology (SNAP): prediction of progression. Neurology 2015;84:508–515.
24. Kaasinen V, Joutsa J, Noponen T, Johansson J, Seppänen M. Effects of aging and gender on striatal and extra-striatal [123I]FP-CIT binding in Parkinson's disease. Neurobiol Aging 2015;36:1757–1763.
25. Tziortzi AC, Haber SN, Searle GE, et al. Connectivity-based functional analysis of dopamine release in the striatum using diffusion-weighted MRI and positron emission tomography. Cereb Cortex 2013;24:1165–1177.
26. Cossette M, Lévesque M, Parent A. Extrastriatal dopaminergic innervation of human basal ganglia. Neurosci Res 1999;34:51–54.
27. Hedreen JC. Tyrosine hydroxylase-immunoreactive elements in the human globus pallidus and subthalamic nucleus. J Comp Neurol 1999;409:400–410.
28. Nobin A, Björklund A. Topography of the monoamine neuron systems in the human brain as revealed in fetuses. Acta Physiol Scand Suppl 1973;388:1–40.
29. Fereshtehnejad S-M, Zeighami Y, Dagher A, Postuma RB. Clinical criteria for subtyping Parkinson's disease: biomarkers and longitudinal progression. Brain 2017;140:1959–1976.
30. Fereshtehnejad S, Montplaisir JY, Pelletier A, Gagnon J, Berg D, Postuma RB. Validation of the MDS research criteria for prodromal Parkinson's disease: longitudinal assessment in a REM sleep behavior disorder (RBD) cohort. Mov Disord 2017;32:865–873.
31. Postuma RB, Adler CH, Dugger BN, et al. REM sleep behavior disorder and neuropathology in Parkinson' s disease. Mov Disord 2015;30:1413–1417.
32. Avenali M, Toffoli M, Mullin S, et al. Evolution of prodromal parkinsonian features in a cohort of GBA mutation-positive individuals: a 6-year longitudinal study. J Neurol Neurosurg Psychiatry 2019; 90:1091–1097.
33. Calabresi P, Castrioto A, Di Filippo M, Picconi B. New experimental and clinical links between the hippocampus and the dopaminergic system in Parkinson's disease. Lancet Neurol 2013;12:811–821.
34. Alberico SL, Cassell MD, Narayanan NS. The vulnerable ventral tegmental area in Parkinson's disease. Basal Ganglia 2015;5:51–55.
35. Pilotto A, Caminiti S, Liguori C, et al. Extra-striatal dopaminergic and serotonergic pathways in Alzheimer's disease: a 123 I-FP-CIT study. Eur J Nucl Med Mol Imaging 2019;46:1642–1651.
36. Ito K, Nagano-Saito A, Kato T, et al. Striatal and extra-striatal dysfunction in Parkinson's disease with dementia: a 6-[18F] fluoro-l-dopa PET study. Brain 2002;125:1358–1365.
37. Sampedro F, Marín-Lahoz J, Martínez-Horta S, et al. Extra-striatal SPECT-DAT uptake correlates with clinical and biological features of de novo Parkinson's disease. Neurobiol Aging 2021;97:120–128.

38. Son S-J, Kim M, Park H. Imaging analysis of Parkinson's disease patients using SPECT and tractography. Sci Rep 2016;6:1–11.

39. Marsden CD. Parkinson's disease. Lancet 1990;335:948–949.

40. Chung KK, Zhang Y, Lim KL, et al. Parkin ubiquitinates the alpha-synuclein-interacting protein, synphilin-1: implications for Lewy-body formation in Parkinson disease. Nat Med 2001;7:1144–1150.

41. Walker Z, Costa DC, Walker RWH, et al. Striatal dopamine transporter in dementia with Lewy bodies and Parkinson disease: a comparison. Neurology 2004;62:1568–1572.

42. Chiasserini D, Paciotti S, Eusebi P, et al. Selective loss of glucocerebrosidase activity in sporadic Parkinson's disease and dementia with Lewy bodies. Mol Neurodegener 2015;10:1–6.

43. Murphy KE, Gysbers AM, Abbott SK, et al. Reduced glucocerebrosidase is associated with increased α-synuclein in sporadic Parkinson's disease. Brain 2014;137:834–848.

44. Parnetti L, Paciotti S, Eusebi P, et al. Cerebrospinal fluid β-glucocerebrosidase activity is reduced in Parkinson's disease patients. Mov Disord 2017;32:1423–1431.

45. Alcalay RN, Levy OA, Waters CH, et al. Glucocerebrosidase activity in Parkinson's disease with and without GBA mutations. Brain 2015;138:2648–2658.

46. Avenali M, Cerri S, Ongari G, et al. Profiling the biochemical signature of GBA-related Parkinson's disease in peripheral blood mononuclear cells. Mov Disord 2021;36:1267–1272.

47. Avenali M, Blandini F, Cerri S. Glucocerebrosidase defects as a major risk factor for Parkinson's disease. Front Aging Neurosci 2020;12:97.

48. Calo L, Wegrzynowicz M, Santivañez-Perez J, Grazia SM. Synaptic failure and α-synuclein. Mov Disord 2016;31(2):169–177.

49. Braak H, Rüb U, Gai WP, Del Tredici K. Idiopathic Parkinson's disease: possible routes by which vulnerable neuronal types may be subject to neuroinvasion by an unknown pathogen. J Neural Transm 2003;110:517–536.

50. Sulzer D, Surmeier DJ. Neuronal vulnerability, pathogenesis, and Parkinson's disease. Mov Disord 2013;28:715–724.

51. Gegg ME, Burke D, Heales SJR, et al. Glucocerebrosidase deficiency in substantia nigra of parkinson disease brains. Ann Neurol 2012;72:455–463.

52. Brockmann K, Schulte C, Deuschle C, et al. Neurodegenerative CSF markers in genetic and sporadic PD: classification and prediction in a longitudinal study. Parkinsonism Relat Disord 2015;21:1427–1434.

53. Stoker TB, Camacho M, Winder-Rhodes S, et al. A common polymorphism in SNCA is associated with accelerated motor decline in GBA-Parkinson's disease. J Neurol Neurosurg Psychiatry 2020;91:673–674.

APPENDIX

Parkinson's Progression Marker Initiative Authors—Steering Committee: Kenneth Marek, MD1; Andrew Siderowf, MD, MSCE2; John Seibyl, MD1; Christopher Coffey, PhD3; Caroline Tanner, MD, PhD4; Duygu Tosun-Turgut, PhD4; Tanya Simuni, MD5; Leslie M. Shaw, PhD6; John Q. Trojanowski, MD, PhD2; Andrew Singleton, PhD7; Karl Kieburtz, MD, MPH9; Arthur Toga, PhD8; Brit Mollenhauer, MD9; Douglas Galasko, MD10; Lana M. Chahine, MD11; Werner Poewe, MD12; Tatiana Foroud, PhD13; Kathleen Poston, MD, MS14; Susan Bressman, MD15; Alyssa Reimer16; Vanessa Arnedo16; Adrienne Clark16; Mark Frasier, PhD16; Catherine Kopil, PhD16; Sohini Chowdhury16; Todd Sherer, PhD16. Study Cores: Leadership Core—Kenneth Marek, MD1; Nichole Daegele1; Clinical Coordination Core—Cynthia Casaceli, MBA17; Ray Dorsey, MD, MBA17; Renee Wilson,17; Sugi Mahes17; Imaging Core—John Seibyl, MD1; Christina Salerno1; Statistics Core—Christopher Coffey, PhD3; Chelsea Caspell-Garcia3; Bioinformatics Core—Arthur Toga, PhD8; Karen Crawford8; Biorepository—Tatiana Foroud, PhD13; Paola Casalin,18; Giulia Malferrari,18; Mali Gani Weisz,19; Avi Orr-Urtreger, MD, PhD19; Bioanalytics Core—John Trojanowski, MD, PhD2; Leslie Shaw, PhD2; Genetics Core—Andrew Singleton, PhD7; Genetics Coordination Core—Tatiana Foroud, PhD13; Pathology Core—Tatiana Foroud, PhD13; Thomas Montine, MD, PhD14; Wearables Core—Tatiana Foroud, PhD13; Advanced Analytics Core—Chris Baglieri,65; Amanda Christini, MD65; Site Investigators—David Russell, MD, PhD1; Caroline Tanner, MD4; Tanya Simuni, MD5; Nabila Dahodwala, MD2; Brit Mollenhauer MD9; Douglas Galasko, MD10; Werner Poewe, MD12; Nir Giladi, MD19; Stewart Factor, DO20; Penelope Hogarth, MD21; David Standaert, MD, PhD22; Robert Hauser, MD, MBA23; Joseph Jankovic, MD24; Marie Saint-Hilaire, MD25; Irene Richard, MD26; David Shprecher, DO27; Hubert Fernandez, MD28; Katrina Brockmann, MD29; Liana Rosenthal, MD30; Paolo Barone, MD, PhD31; Alberto Espay, MD, MSc32; Dominic Rowe, BSc, MBBS33; Karen Marder, MD, MPH34; Anthony Santiago, MD35; Susan Bressman, MD36; Shu-Ching Hu, MD, PhD37; Stuart Isaacson, MD38; Jean-Christophe Corvol, MD39; Javiar Ruiz Martinez, MD40; Eduardo Tolosa, MD41; Yen Tai, MD42; Marios Politis, MD, PhD43; Coordinators—Debra Smejdir1; Linda Rees, MPH1; Karen Williams3; Farah Kausar4; Karen Williams5; Whitney Richardson2; Diana Willeke9; Shawnees Peacock10; Barbara Sommerfeld, RN, MSN20; Alison Freed21; Katrina Wakeman22; Courtney Blair, MA23; Stephanie Guthrie, MSN24; Leigh Harrell23; Christine Hunter, RN24; Cathi-Ann Thomas, RN, MS25; Raymond James, RN25; Grace Zimmerman26; Victoria Brown27; Jennifer Mule BS28; Ella Hilt29; Kori Ribb30; Susan Ainscough31; Misty Wethington32; Madelaine Ranola33; Helen Mejia Santana34; Juliana Moreno35; Deborah Raymond36; Krista Speketer37; Lisbeth Carvajal38; Stephanie Carvalo39; Ioana Croitoru40; Alicia Garrido, MD41; Laura Marie Payne, BSc42; Industry and Scientific Advisory Board—Veena Viswanth, PhD44; Lawrence Severt, PhD44; Maurizio Facheris, MD45; Holly Soares, PhD45; Mark A. Mintun, MD46; Jesse Cedarbaum, MD47; Peggy Taylor, ScD48; Kevin Biglan, MD49; Emily Vandenbroucke, PhD50; Zulfiqar Haider Sheikh50; Baris Bingol51; Tanya Fischer, MD, PhD52; Pablo Sardi, PhD52; Remi Forrat52; Alastair Reith, PhD53; Jan Egebjerg, PhD54; Gabrielle Ahlberg Hillert54; Barbara Saba, MD55; Chris Min, MD, PhD56; Robert Umek, PhD57; Joe Mather58; Susan De Santi, PhD59; Anke Post, PhD60; Frank Boess, PhD60; Kirsten Taylor60; Igor Grachev, MD, PhD61; Andreja Avbersek, MD62; Pierandrea Muglia, MD62; Kaplana Merchant, PhD63; Johannes Tauscher, MD64.

Affiliations: 1 Institute for Neurodegenerative Disorders, New Haven, CT; 2 University of Pennsylvania, Philadelphia, PA; 3 University of Iowa, Iowa City, IA; 4 University of California, San Francisco, CA; 5 Northwestern University, Chicago, IL; 7 National Institute on Aging, NIH, Bethesda, MD; 8 Laboratory of Neuroimaging (LONI), University of Southern California, Los Angeles, CA; 9 Paracelsus-Elena Klinik, Kassel, Germany; 10 University of California, San Diego, CA; 11 University of Pittsburgh, Pittsburgh, PA; 12 Innsbruck Medical University, Innsbruck, Austria; 13 Indiana University, Indianapolis, IN; 14 Stanford University, Stanford, CA; 15 Mount Sinai, New York, NY; 16 The Michael J. Fox Foundation for Parkinson's Research, New York, NY; 17 Clinical Trials Coordination Center, University of Rochester, Rochester, NY; 18 BioRep, Milan, Italy; 19 Tel Aviv Medical Center, Tel Aviv, Israel; 20 Emory University of Medicine, Atlanta, GA; 21 Oregon Health and Science University, Portland, OR; 22 University of Alabama at Birmingham, Birmingham, AL; 23 University of South Florida, Tampa, FL; 24 Baylor College of Medicine, Houston, TX; 25 Boston University, Boston, MA; 26 University of Rochester, Rochester, NY; 27 Banner Research Institute, Sun City, AZ; 28 Cleveland Clinic, Cleveland, OH; 29 University of Tuebingen, Tuebingen, Germany; 30 Johns Hopkins University, Baltimore, MD; 31 University of Salerno, Salerno, Italy; 32 University of Cincinnati, Cincinnati, OH; 33 Macquarie University, Sydney Australia; 34 Columbia University, New York, NY; 35 The Parkinson's Institute, Sunnyvale, CA;

36 Beth Israel Medical Center, New York, NY; 37 University of Washington, Seattle, WA; 38 Parkinson's Disease and Movement Disorders Center of Boca Raton, Boca Raton, FL; 39 Hospital Pitie-Salpetriere, Paris, France; 40 Hospital Donostia, San Sebastian, Spain; 41 Hospital Clinic de Barcelona, Barcelona, Spain; 42 Imperial College London, London, United Kingdom; 43 King's College London, London, United Kingdom; 44 Allergan, Dublin, Ireland; 45 Abbvie, North Chicago, IL; 46 Avid Radiopharmaceuticals, Inc., Philadelphia, PA; 47 Biogen Idec, Cambridge, MA; 48 BioLegend, Dedham, MA; 49 Eli Lilly and Company, Indianapolis, IN; 50 GE Healthcare, Princeton, NJ; 51 Genentech, San Francisco, CA; 52 Genzyme Sanofi, Cambridge, MA; 53 GlaxoSmithKline, Brentford, United Kingdom; 54 H. Lundbeck A/S, Copenhagen, Denmark; 55 Institut de Recherches Internationales Servier, Neuilly-sur-Seine, France; 56 Merck and Co., Kenilworth, NJ; 57 Meso Scale Diagnostics, Rockville, MD; 58 Pfizer Inc., Cambridge, MA; 59 Piramal Group, Mumbai, India; 60 F. Hoffmann-La Roche Limited, Basel, Switzerland; 61 Teva Pharmaceutical Industries, Petah Tikva, Israel; 62 UCB Pharma, Brussels, Belgium; 63 TransThera Consulting, Portland, OR; 64 Takeda, Osaka, Japan; 65 Blackfynn, Philadelphia, PA

Supporting Data

Additional Supporting Information may be found in the online version of this article at the publisher's web-site.